High Redshift X-ray Jets detections with Chandra

Aneta Siemiginowska (CfA), Kathryn McKeough (CMU), Teddy Cheung (NRL), Vinay Kashyap (CfA), Nathan Stein (UPenn), David Van Dyk (Imperial College) et al.

ABSTRACT:
We present results from morphological studies of X-ray jets observed in the two highest redshift quasars with Chandra X-ray Observatory. We apply a novel computational technique to work with low counts Poisson images and separate jet emission from a strong quasar core. The X-ray angular resolution matches the resolution of the radio maps allowing for direct studies of the location of X-ray and radio jet emission. We attempt to constrain the parameters of the jet emission process and estimate a jet power for these jets.

The two highest redshift X-ray Jets resolved by Chandra

CXC-Press Release Image

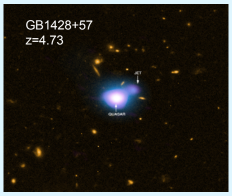

Cheung et al 2012

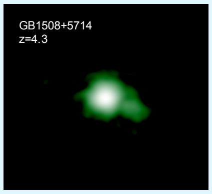

Siemiginowska et al 2003

Overview

- Large scale jets signal an ongoing jet and radio source activity. They can provide important constraints on the physical processes governing the black hole growth and evolution.
- The CMB energy density scales as $(1+z)^4$ and at high-z can impact the overall radio structures including jets.
- Only a handful of X-ray jets has been observed with Chandra. The detections of typically fainter jets in the vicinity of a strong quasar emission is non trivial.
- We use LIRA (Low-counts Image Reconstruction and Analysis) in our analysis of the two highest redshift resolved by Chandra to "remove" a point-like quasar emission and discern the remaining X-ray emission associated with the diffuse and jet structures in these data.

Chandra X-ray Observations

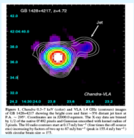

Cheung et al. 2012

GB 1428+4217, z = 4.72
Chandra ACIS-S
Exposure time: 11.7ksec
X-ray jet: 20.3±0.4 counts
Core: 2200±47 counts

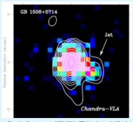

Chandra X-ray image of GB 1508+5714 (color) with VLA 1.4 GHz image overlaid.. The radio image restored with the uniformly weighted beam (1"52 × 1"03 at P.A. = -4°44). The lowest contour plotted is 0.2 mJy beam-1 and subsequently spaced by factors of 2.

Cheung et al 2004
Siemiginowska et al 2003

GB 1508+5714 z=4.3
Exposure time: 80 ksec
X-ray jet: 131.0±11.4 counts
Core: 4730±68 counts

X-ray Image Analysis with LIRA

LIRA:
Bayesian Statistical Model with Two Poisson processes:
1/ Known Emission
2/ Unknown Secondary Structure
Markov Chain Monte Carlo (MCMC) simulates multiple iterations under the data and the known emission model.

Statistical significance of the existence of secondary structures are computed by comparing the multiscale residual over the pre-defined regions to similarly computed residuals from simulated images which definitely lack the features.

INPUT:
Model Image for the known emission
Simulated Data based on the Known Model
Observed Data
PSF Image

LIRA Returns:
Many simulated images of the residual from MCMC runs.

Simulated Quasar Model

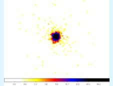

Chandra PSF

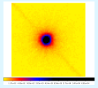

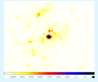

Output Image from LIRA showing the residuals based on the Simulated Quasar Model.

Results

GB1428+4217

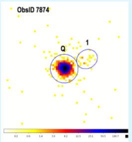

Chandra Data

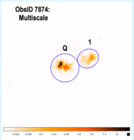

Average Simulated Image from LIRA showing the residuals after accounting for the core and background emission.

Table 1: Parameters for each quasar core and jet regions.

ObsID	Region	Number of Pixels	Photon Count	Exp. Bkg. Count	p-value ($\hat{u}$)	Signif. ($\alpha = 0.01$)	Avg. τ_1
7874	Q	181	2157	1.01	0.01	Yes	69.51
	1	91	19	0.51	0.01	Yes	4.04
	C	3824	60	21.25	1.00		1.85
2241	Q	72	4730	2.40	0.01	Yes	78.35
	1	79	131	2.63	0.01	Yes	111.35
	C	3945	403	131.50	0.01	Yes	48.60

– Q - quasar core, 1 - numbering for identified jet regions based on radio data, C - a region complementary to the quasar and a jet (the entire image minus the quasar core and jet regions)

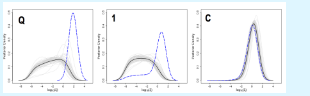

Posterior densities for each regions based on the known model simulations (grey) and the data (blue)

Q - quasars, 1 - jet, C - the complementary region (outside Q and 1)

For both Sources:

- The X-ray jet emission in jet regions 1 is highly significant as shown in the posterior density figures.
- There is a significant residual emission within the quasar core, which might be due to the uncertainties in the PSF, or related to a non-point nature of the X-ray emission within the core regions.
- Radio morphology of the jet on sub-arcsec scales is complex and the X-ray emission associated with these small scale radio emission might also be complex, although unresolved.

GB1508+5714

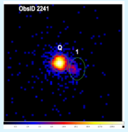

Chandra Data

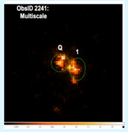

Average Simulated Image from LIRA showing the residuals after accounting for the core and background emission.

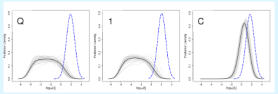

Posterior densities for each regions based on the known model simulations (grey) and the data (blue)

Q - quasars, 1 - jet, C - the complementary region (outside Q and 1)

Radio Properties

Radio Morphology on large scales: jet projected > 10 kpc

Resolution matching the Chandra subarcsec capabilities

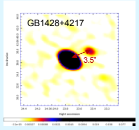

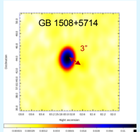

Radio Morphology on small scales: jet projected < 1kpc

Scales Unresolved with Chandra

2.3 GHz ~200 pc
3 knots :PA from -96° to -117°
jet-to-counter jet ratio ~ 7

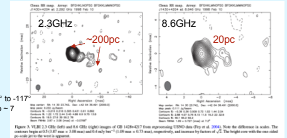

Cheung et al 2012

Physical Parameters

The flux of the X-Ray and Radio emissions

ObsID	Region	X-Ray Flux 10^{-15}(erg/s/cm^2)	Radio Flux 10^{-15}(erg/s/cm^2)	(X-ray/Radio)
2241	Q	1360.00	2.54	535.4
	1	37.80	0.02	1890
7874	Q	65.60	2.20	29.8
	1	0.58	0.02	29.

Observed X-ray Jet Luminosities:
GB1508 1.0e47 erg/s
GB1428 3.2e47 erg/s

Table 1: X-ray Spectral Fits for Quasar and Jet Regions

source	Region (1)	Norm (2)	Γ_X (3)	$N_H(z)$ (4)	F(0.5-2 keV) (5)	F(2-10 keV) (6)	C-stat
1428+422	Q	$239.52^{+6.61}_{-6.51}$	$1.36^{+0.04}_{-0.04}$	–	$55.39^{+1.48}_{-1.46}$	$169.50^{+9.81}_{-11.62}$	528.73
1428+422	Q	$262.72^{+15.48}_{-14.54}$	1.44±0.06	$2.32^{+1.29}_{-1.26}$	$60.68^{+3.19}_{-3.63}$	$162.72^{+16.92}_{-16.52}$	525.29
1428+422	1	$2.39^{+0.71}_{-0.59}$	$1.64^{+0.39}_{-0.38}$	–	$0.56^{+0.13}_{-0.15}$	$1.07^{+0.94}_{-0.53}$	95.17
1508+572	Q	$64.36^{+1.11}_{-1.10}$	$1.55^{+0.02}_{-0.02}$	–	$14.60^{+0.23}_{-0.24}$	$33.53^{+1.49}_{-1.39}$	522.54
1508+572	Q	$65.50^{+2.31}_{-2.03}$	1.56±0.04	< 0.57	$14.80^{+0.54}_{-0.53}$	$33.35^{+2.41}_{-2.30}$	522.20
1508+572	1	$2.14^{+0.20}_{-0.19}$	$1.83^{+0.15}_{-0.14}$	–	$0.48^{+0.04}_{-0.05}$	$0.71^{+0.20}_{-0.17}$	239.02

Notes – (1) Regions. – (2) Norm [10^{-6}] photons cm^{-2} s^{-1}. – (4) Intrinsic absorption in 10^{22} cm−2.– (5, 6) Fluxes [10^{-14}] erg cm^{-2} s^{-1} – The N_H was frozen at the Galactic values in fitting the simple power law or power law with intrinsic absorption. The fluxes in the table are corrected for absorption and are calculated in the observer frame (i.e. not k-corrected).

Summary and Conclusions

- We applied LIRA to the Chandra observations of the two highest redshift X-ray jet detected to date.
- Both jets are at the small angle to our line of sight < 20° and their small X-ray emission of ~3.5 arcsec implies the length of > 70 kpc.
- CMB energy density at z > 4.3 is > 790 times greater than at z=0 and can influence these jets dramatically.
- The current observations suggest that the two high-z jets maybe slower due to the interaction with the environment or due to origin of their activity.
- The image analysis indicate a possible non-point line X-ray emission within the core regions.
- In GB1508+5714 the X-ray emission extends beyond the radio jet structure showing the bend.
- Observations of larger sample of known high redshift radio jets in X-ray is needed to understand the X-ray properties of the jets and environment of radio loud quasars.

References

Cheung, C.C. 2004, Radio Identification of the X-Ray Jet in the z=4.3 Quasar GB 1508+5714, ApJL, 600, L23
Cheung, C.C. et al., 2012, Discovery of a Kiloparsec-scale X-Ray/Radio Jet in the z = 4.72 Quasar GB 1428+4217, ApJ,L, 756, L20
Siemiginowska et al 2003, An X-Ray Jet Discovered by Chandra in the z=4.3 Radio-selected Quasar GB 1508+5714, ApJ,598, L19
McKeough et al 2014, Bayesian Multi-scale Analysis of X-ray jet features at high redshift, AAS
Stein et al 2014, Significance of unspecified structures in Poisson Images - in preparation

LIRA: https://github.com/astrostat/LIRA

Acknowledgments

This research is funded in part by NASA contract NAS8-03060 and through Chandra Awards GO1-12145X, GO1-12124X and Fermi Award NNX10AO60G.